COMPDYN 2011
III ECCOMAS Thematic Conference on
Computational Methods in Structural Dynamics and Earthquake Engineering
M. Papadrakakis, M. Fragiadakis, V. Plevris (eds.)
Corfu, Greece, 25–28 May 2011

INNOVATIVE MULTIFUNCTIONAL REINFORCEMENT TECHNOLOGY FOR MASONRY BUILDINGS: NUMERICAL VALIDATION AND DAMAGE DETECTION INVESTIGATION

C. Fuggini[1*], E. Chatzi[2], D. Zangani[3], T. B. Messervey[3]

[1]Industrial Innovation Division, D'Appolonia S.p.A.
Via San Nazaro 19, 16145 Genova (Italy)
clemente.fuggini@dappolonia.it

[2] Institute of Structural Engineering, ETH Zürich
Wolfgang-Pauli-Strasse 15, CH-8093 Zürich
chatzi@ibk.baug.ethz.ch

[3] Industrial Innovation Division, D'Appolonia S.p.A
Via San Nazaro 19, 16145 Genova (Italy)
donato.zangani@dappolonia.it, thomas.messervey@dappolonia.it

Keywords: Damage Detection, Masonry Buildings, Numerical Simulations, Multifunctional textiles, Genetic Algorithm.

Abstract. *This paper reports the outcomes of an experimental test campaign for the validation of the performance of a seismic reinforcing strategy of masonry buildings based on the full covering of the building by means of an innovative multifunctional technical textile. This innovative solution, the "Composite Seismic Wallpaper" is made of glass and polymeric fibres in a multiaxial textile structure featuring embedded fiber optics sensors which is connected to the substrate using a special cementitius matrix. The composite obtained is multifunctional in the sense that on one side it reinforces the structure, increasing its capacity to resist to seismic events, and on the other side, it provides localized and distributed static and dynamic measurements before, during and after a seismic event, by means of the integrated sensors. Recently "Seismic Wallpaper" has been full-scale tested as reinforcement of a two-story stone building. The reinforced building has been tested in shaking table tests campaign to prove the feasibility of the distributed and passive reinforcing solution and to investigate the reliability, in detecting the building dynamics, of Fiber Bragg Grating (FBG) sensors embedded in the textile fabric. Sensors measurements recorded during hammer shock tests and shaking tables have been analyzed towards a modal identification of the building modal parameters. This paper first presents the building modelling by means of finite elements analyses, then describes the buildings dynamics as characterized from experimental tests, finally proposes a methodology for damage detection by means of an inverse problem approach that combines an evolutionary method (Genetic Algorithms) and a plain FEM simulation based model for the localization of damage.*

1 INTRODUCTION

Masonry structures are complex structures, as they are constituted by non-homogeneous materials (i.e., bricks, stones, mortar), they exhibit in-plane and out-of-plane failure mechanism which are prevalently sliding, flexural and shear type and they are prone to damages and fragile collapses when excited by dynamic loads. In particular when excited by seismic loads, masonry structures are subjected to cracks propagations which progressive lead the structure to collapse. In which way the structural collapse due to a seismic action may be avoided or move away it is an open point of discussion in the scientific community as many and different techniques may be considered and may be reliable, depending on the characteristics of the input dynamic load and on the different parameters which may be involved.

Most of masonry buildings are old buildings which have not been designed against earthquakes but only to resist to gravity loads and the effect of seismic loads were. During earthquake, seismic loads introduce severe in-plane and out-of-plane forces to unreinforced masonry buildings, many of them, collapse in out-of-plane bending due to lack of reinforcement.

When dealing with the reinforcement of masonry building against natural hazards such as earthquakes, all the aforementioned considerations should be taken into account.

To this aim, the techniques investigated and adopted for the reinforcement of masonry building aimed at providing more flexibility and ductility to the masonry walls and at preventing out-of-plane and/or in-plane failing mechanism by means of guaranteeing a stronger and reliable confinement and connection of the masonry walls. In general the objective of the retrofitting should be to enhance the earthquake resistance of masonry structures in order to avoid its failure in brittle manner.

Following a short review of the historic developments of masonry reinforcement solutions, as they are reported in the more important codes, guidelines and handbooks, they can be divided in traditional (i.e. conventional) techniques and innovative techniques.

Traditional methods of strengthening are intervention techniques to remedy structural deficiency by means of local or overall modification of damaged or undamaged elements (repair, strengthening or full replacement). The conventional methods are:

- Addition of new structural elements (bracings system; steel, timber or reinforced concrete belts);
- Injection of cement or epoxy grout into cracks to fill cracks and voids;
- Local replacement of damaged masonry bricks and reassembling them with improved mortar and proper reinforcement (reinforcing bars);
- Improving the connection between intersecting walls through construction of a reinforced concrete belt, addition of steel plates in the bed-joints, or insertion of inclined steel bars in drilled holes;
- Strengthening and stiffening of horizontal diaphragms;
- Addition of steel ties (along or transversely to the walls, external or within holes drilled in the walls) to connect walls and to improve the overall behaviour of a masonry building;
- Strengthening of rubble core masonry walls by cement grouting;
- Strengthening of walls by confinement with reinforced concrete jackets or steel profiles.

Among the innovative techniques, three main areas can be identified:

- Seismic Isolation (i.e., base isolation);

- Fiber Reinforced Polymers materials;
- Energy Dissipation Devices (as example passive control devices based on Shape Memory Alloy (SMA).

Furthermore seismic retrofitting of most of masonry structures requires compliance with restrictive constraints related to the preservation of the original structural features. Any conceived intervention must achieve structural performance yet still respect the appearance and structural mechanism of the original and be as minimally invasive as possible. Therefore, traditional retrofit strategies may not be suitable for such purposes, and structural engineers need to develop specific techniques. Innovative materials, such as textile composites may be helpful with respect to these issues. In fact composites provide a non-intrusive technique to provide reinforcing strength to a structure and are feasible for applications which include localized crack repair, the reinforcement of critical walls, or the wrapping of existing columns.

In addition, conventional methods add significant mass to the structure, encroach upon the available working space, and adversely affect the aesthetics of the repaired portions. The extra mass added to the structure during strengthening increases the earthquake induced inertia forces and may necessitate the strengthening of the footings. Also from this point of view solution based on innovative composites materials should be adopted. In particular Fiber Reinforced Polymer (FRP) composites offer a viable alternative to the conventional strengthening methods as they offer: high strength to weight ratio, resistance to electro-chemical corrosion, larger creep strain, good fatigue strength, potential for decreased installation costs and repairs, non-magnetic properties.

In the field of strengthening, textiles composite materials combined with mortars were used recently as a means of increasing the strength of masonry, either in diagonal compression [5] or in uniaxial compression through confinement [6, 7]. Studies have dealt with strengthening of: walls, through external prestressing [8]; columns, through confinement [9]; walls subjected to in-plane or out-of-plane loading, through externally bonded strips or overlays [10]; walls through near-surface mounted reinforcement [11].

In general solutions of this type are based on narrow fabric/sheets strips of FRP composite materials (carbon or glass fibers based) glued by means of a resin on masonry walls in localized position. Strips reinforcement solutions based textile materials represent an efficient reinforcement strategy. However, striped reinforcements of masonry walls they may excessively increasing the walls stiffness and may create stress concentrations, which may change the way the structure is responding to actions such as earthquakes and may transfer to weak zones the capacity of the wall to resist.

A step further should be on one side to investigate innovative materials and on the other side to adopt new strategy for the reinforcement solution. An answer to the first need could be to adopt multi-axial composite textiles, while to address the second issue one strategy is to move from localized (i.e. striped) reinforced solutions to global full-cover solutions.

Both issues have been addressed within the EU funded project Polytect ("Polyfunctional Technical Textiles for Protection against Natural Hazard") which developed an innovative concept for the reinforcement and protection of masonry buildings against earthquakes by means of a multi-axial composite based skin for the full-covering of masonry walls. This solution, in the following "Composite Seismic Wallpaper", was awarded at the JEC2010, as innovative product in the Building and Construction Category.

The Composite Seismic Wallpaper is an innovative solution, as it not only provides reinforcement capability by means of a multi-axial FRP, but also because it provides monitoring capability by means of fiber optics sensors embedded into the textile since the manufacturing

stage. The wallpaper represents a progress beyond the state of the art of masonry building reinforcement solutions using textile materials because:

- It reinforces the building by increasing the structural strength;
- It increases the building's ductility, without stiffness increase;
- It monitors the building structural health by means of strain measurements;
- It detects the damage in the building walls.

Furthermore, the aforementioned characteristics of the wallpaper make it suitable for reinforcing application in compliance with Italian and EU codes referring to this topic. In particular it can be stated that the integration of a monitoring system into a reinforcing solution is needed since there is a lack of information on long-term behaviour of reinforcing applications with textiles materials [12]. In fact from paragraph 5.8.5 "Monitoring of the strengthening system" of [12] it can be extracted what follows: "Due to the poor availability of data regarding long term behavior of FRP systems… it is recommended to perform appropriate monitoring …. to keep the following parameters under control: Temperature… humidity…. displacements and deformations… Potential damage of fibers…. Extensions of defects and delamination…". The seismic wallpaper is an effective and reliable answer to this need.

2 THE COMPOSITE SEISMIC WALLPAPER

From a components point of view, the wallpaper consists of:

- Multi-axial, warp-knitted, AR-glass and Polypropylene (PP) fibres, which constitute the composite fibers (Figure 1);
- Nanoparticle enhanced coatings for the textile fabric;
- Nanoparticle enhanced mortar (the matrix of the composite) to bond the textile to the structure;
- Fibre optic sensors (Figure 2);
- An interrogation system to acquire data from the sensor-embedded textile-mortar composite.

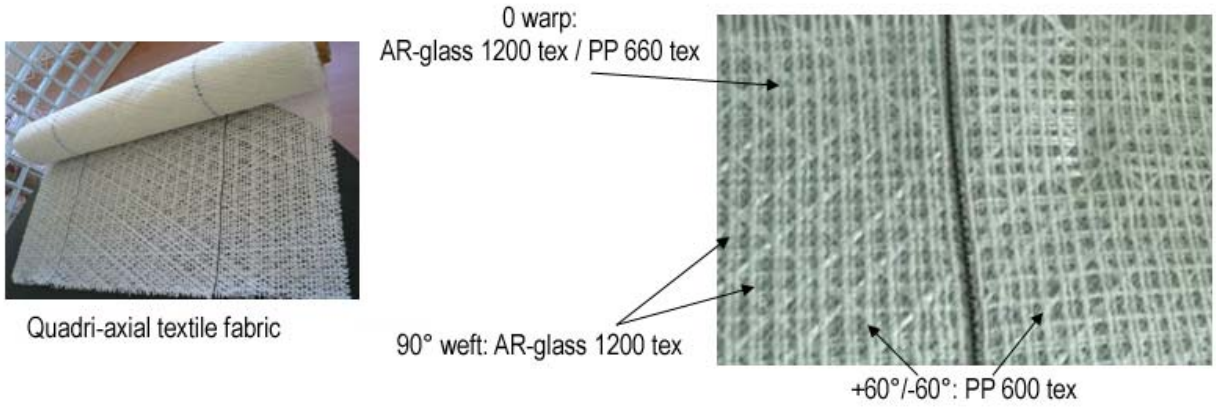

Figure 1: Quadric-axial technical textile

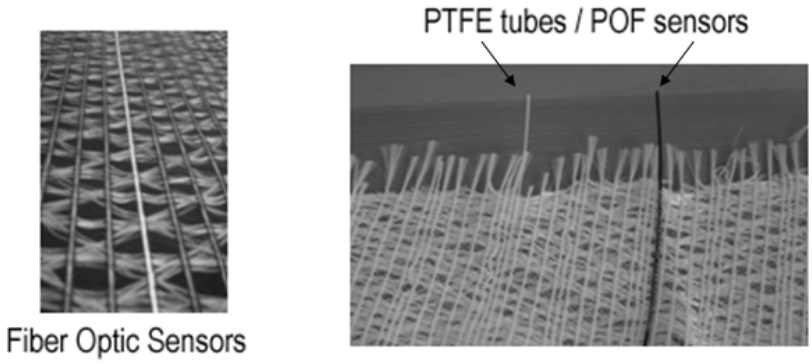

Figure 2: Fiber optic sensors embedded textile

The realization of these components, their processing, and application onto real structures has been investigated within the Polytect project and tested in full-scale seismic tests at the European Centre for Training and Research in Earthquake Engineering (Eucentre) under the "Seismic Engineering Research Infrastructures for European Synergies" (Series) initiative.

An un-reinforced two stories stone building (Figure 3) has been identified to be suitable for the full-scale application of the seismic wallpaper reinforcing solution.

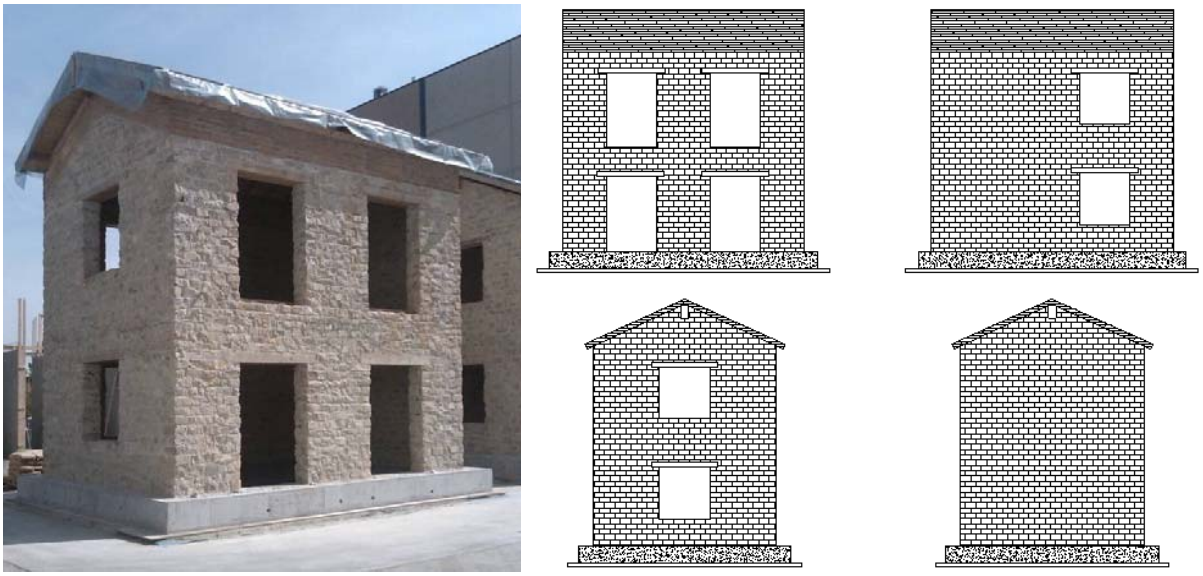

Figure 3: 3D View of the un-reinforced stone building (left); N-S-W-E fronts (right)

The building is made of natural stones which mechanical properties. The roof is wood made and is simply supported to the walls. Its structure is made of longitudinal and transversal beams. The building is 5.80m long (X direction), 4.40m width (Y direction) and 5.80m high (Z direction). The foundation (40cm tall) is made of concrete, while a wood slab is realized in between the first and the second story (Figure 4). The mechanical properties of the materials constituting the building are reported in Table 1 below.

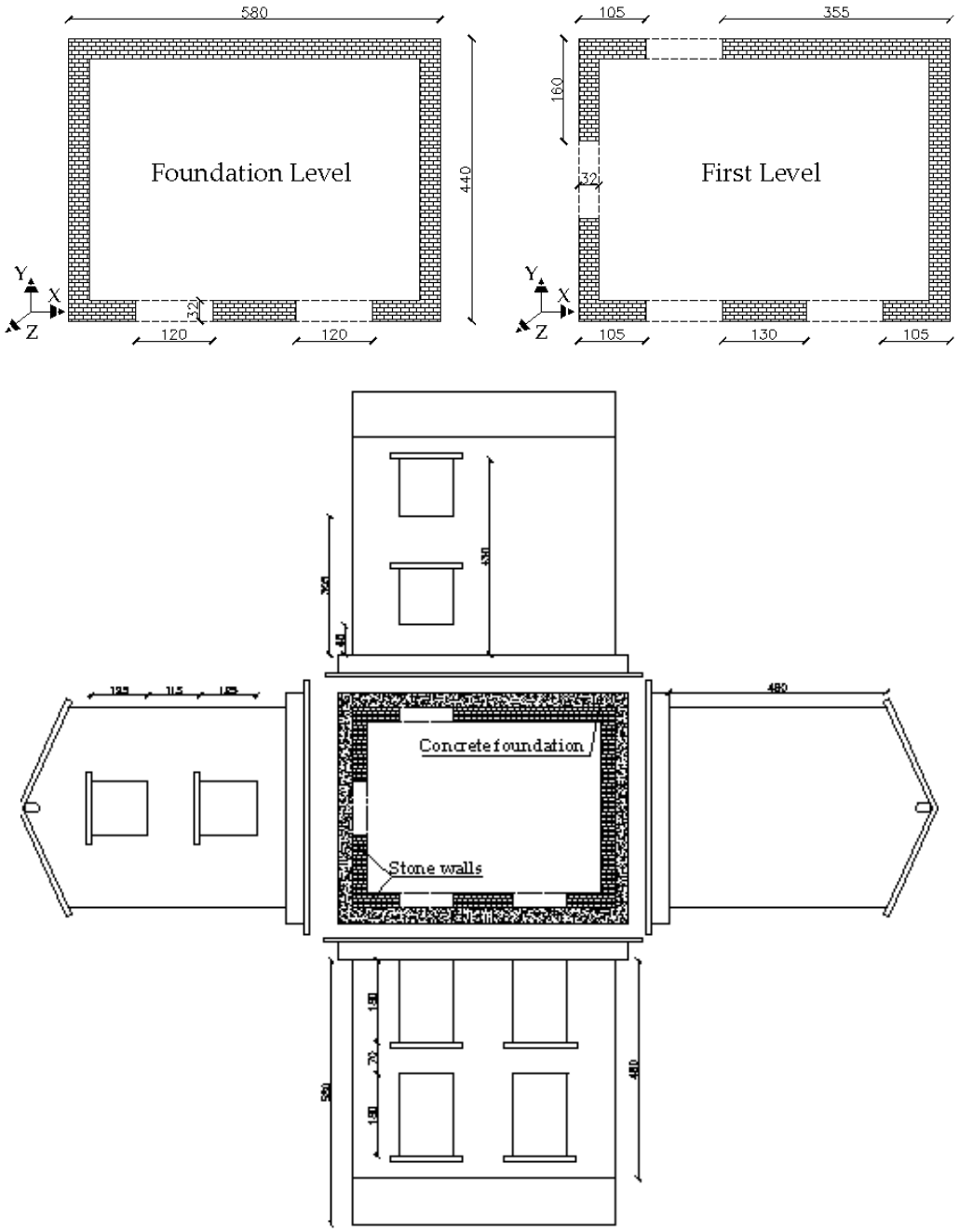

Figure 4: The un-reinforced stone building: plan view (top); sectional view (bottom)

Density	2579 kg/m3
Young Modulus $E_{x,y}$	2550 MPa
Young Modulus E_z	2550 MPa
Poisson Coefficient ν	0.4
Shear Modulus $G_{xy}=G_{xz}$	840 MPa
Shear Modulus G_{yz}	840 MPa
Maximum compression stress σ_c	3.28 MPa
Maximum tensile stress σ_t	0.137 MPa
Density	750 kg/m3

Young Modulus E	11000 MPa
Poisson Coefficient ν	0.2
Density	2400 kg/m3
Young Modulus E	30000 MPa
Poisson Coefficient ν	0.2

Table 1: Mechanical properties of material adopted in the un-reinforced building: natural stone (top); wood (middle); concrete (bottom)

Afterwards the stone building has been reinforced by means of the seismic wallpaper, which has been applied to the stone walls using a mortar compound, constituted of an epoxy-cementitious matrix combined with nanoacrylic polymers. The cohesion of the masonry part of the structure is achieved by using this matrix of ductile type, which benefit is a damping effect through load distribution. The matrix also protects the glass fibres against the alkaline environment of the plaster. In detail (Figure 5), the reinforcement has been realized by means of further steps:

- first the matrix has been applied fresh to the walls external surface, making the surface as smoothed as possible;
- then the textile was rolled out from the roof, applied to the fresh mortar, pushed against it till a mortar penetration into the textile fabric structure was reached,
- finally a second layer of matrix was applied to externally cover the textile.

This procedure guarantees that a perfect bonding between masonry, matrix and textile is reached.

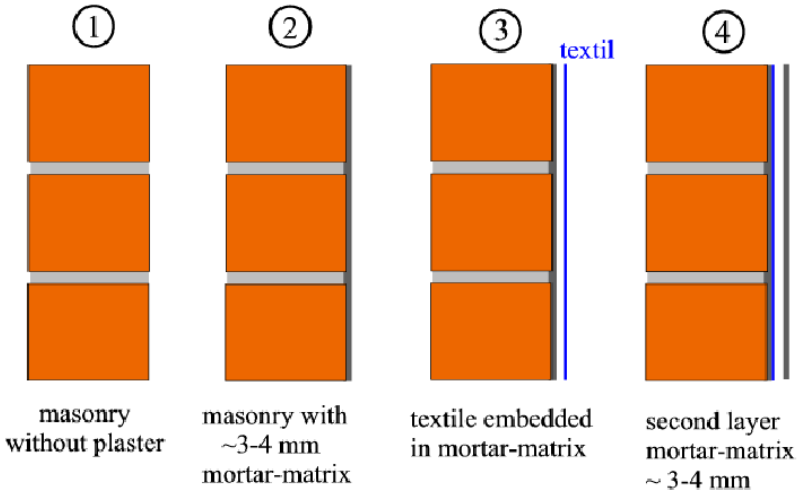

Figure 5: Seismic Wallpaper application procedure

The result is the reinforced building depicted in Figure 6, the grey colour is given by the outer cementitious matrix layer, covering the quadric-axial textile, which mechanical properties are reported in Table 2 below.

Figure 6: View of the reinforced building

Density	2000 kg/m3
Young Modulus E_x	40000 MPa
Young Modulus $E_{y,z}$	32000 MPa
Poisson Coefficient ν_{xy}	0.14
Poisson Coefficient $\nu_{xz,\ yz}$	0.2
Shear Modulus G_{xy}=G_{xz}= G_{xz}	4500 MPa
Maximum tensile stress σ_t	40 MPa
Maximum shear stress σ_s	10 MPa

Table 2: Mechanical properties of the quadric-axial textile

Before and in parallel with the experimental tests carried on at the Eucentre by means of subsequent seismic events of increasing intensity applied to the base of the reinforced building mounted on an uni-axis shaking table, numerical simulation were mandatory to assess the effectiveness of the reinforcing solution, to predict the building behavior and to achieve knowledge of the textile response to dynamic loads.

This process has been developed and is presented within this paper by means of subsequent steps/analysis which from preliminary finite element model (FEM) and numerical investigations of the un-reinforced building, the building as damaged and the reinforced building, is aimed at describing a proper method for the simulation of the inelastic behavior of this innovative technical textile concept.

3 PRELIMINARY FE ANALYSIS AND COMPARISON WITH EXPERIMENTAL RESULTS

Preliminary numerical simulations have been carried out with the aim of understanding the structural behavior of the un-reinforced building (URB) as a mean of comparison with the reinforced building (REB) behavior. It is worth noting that these simulations did not account for any micro-scale modeling of the seismic wallpaper (i.e. of the quadric-axial textile) since this optimization has been performed in a further step of the study, as reported in chapter4. Here

modal as well as non-linear static and non-linear dynamic analyses have been conceived towards the prediction of the building dynamics in terms of modal parameters (frequencies, damping and mode shapes) for both the URR and the REB. The simulations aimed at understanding the benefits of a full-cover solution with respect to traditional strips reinforcing solution in terms of stress distribution, in ductility capability and in dissipation of energy capacity.

The Ansys software has been identified as suitable for the numerical analyses. The classical implicit formulation has been adopted; the Newton-Raphson iteration algorithm has been implemented. A solid model has been conceived for modeling the stone walls, while shell elements have been used for meshing the wood slab and the wood roof. According to the requirements of the analysis performed the Solid45 and/or the Solid65 element have been used for the stone walls, in particular: the Solid45 element (3-D Structural Solid) has been used when simulating a modal analysis, while the Solid65 element has been judged more suitable, due to its nonlinear capability, to be adopted when performing a non-linear analysis. The seismic wallpaper has been modeled as an equivalent homogeneous lamina by means of shell elements, accounting for both the quadri-axial textile (with fiber oriented at 0°, 90° and ±60°) and the epoxy-cementitious matrix. A perfect contact in between the solid elements (representing the wall stones) and the shell elements for the wallpaper has been simulated. Shell43 4node non-linear element has been chosen, with both bending and membrane capability.

The FEM of the URB as well as of the REB are shown in Figure 7 below.

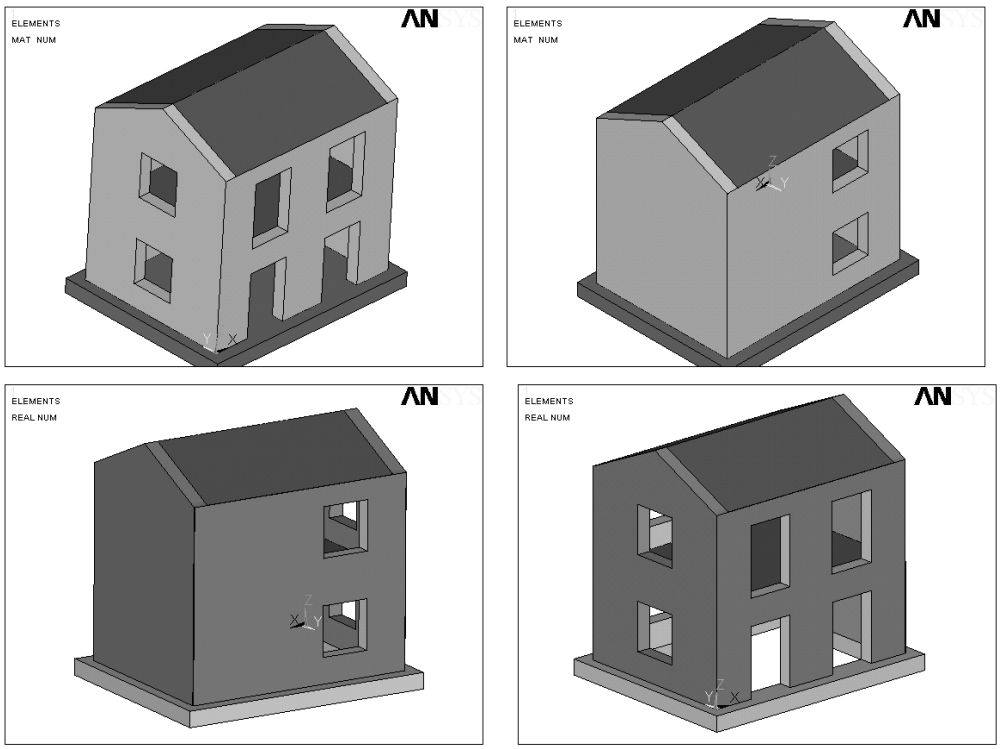

Figure 7: FEM of the un-reinforced building (top) and of the reinforced building (bottom)

3.1 Modal Analysis

The modal analysis aims at predicting the building natural frequencies and modes shapes to be compared with the same parameters identified from experimental tests. In addition a

comparison between the un-reinforced and the reinforced building natural frequencies, as calculated from numerical simulations, is also realized.

Figures 8 reports the displacements field mode shapes for the 1st, the 2nd and the 3rd mode, for the URB and the REB respectively. Table 3 summarizes the results for both configurations in terms of calculated natural frequencies.

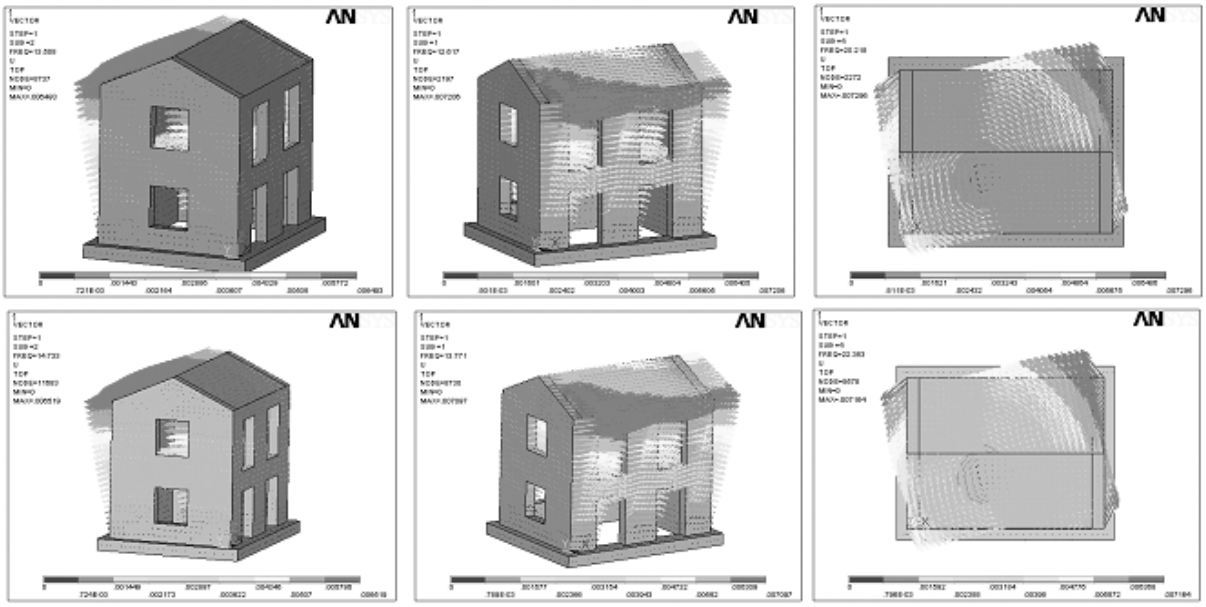

Figure 8: Modal analysis results of the URB (top) and the REB (bottom). Displacements field of the 1st (left plot), 2nd (middle plot) and 3rd (right plot) mode shape

Mode	URB Frequency [Hz]	REB Frequency [Hz]
1st (translation in Y)	13.51	14.73
2nd (translation in X)	12.62	13.77
3rd (torsional)	20.22	22.35

Table 3: Modal analysis results

The results calculated from numerical simulations have been then compared with those coming from experimental ambient vibrations tests carried on for both the URB and the REB. The aim here is to calibrate the numerical model and to give an estimate of the changes the reinforcement is given in terms of the building dynamics.

Four three-axis Geophones have been located on the parapet of the building windows according to the set-up configuration showed of Figure 9. Two sets of ambient vibrations have been recorded at a sampling rate of 265Hz for around half an hour. Two minutes of measurements have been extracted from the global records for both ambient vibration sets. The Operational Modal Analysis (OMA) has been carried on by processing with suitable algorithms (Natural Excitation Technique combined with the Eigensystem Realization Algorithm: Next-ERA) the two minutes records.

Far from the scope of this study, the experimental process is not described in detail. The results are reported in terms of identified natural frequencies for comparison with the numerical calculations (Table 4). The correlation between experimental and numerical natural frequencies is also highlighted in Figure 10, with reference to the URB.

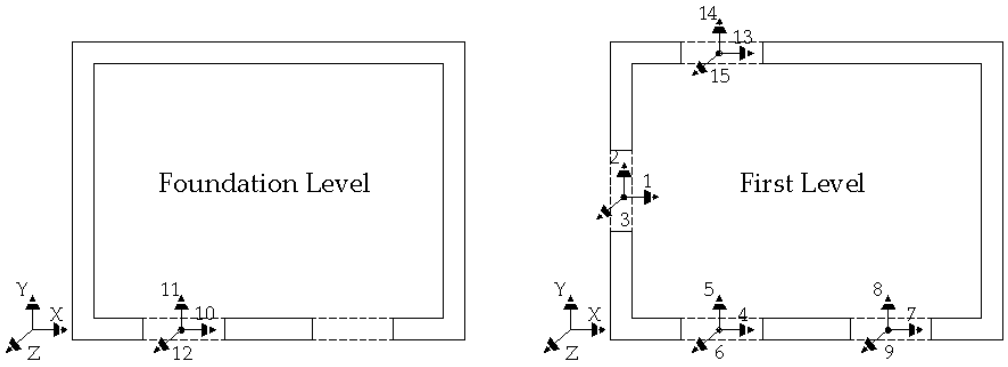

Figure 9: Experimental Ambient Vibration tests sensor set-up

Mode	URB Frequency [Hz]		REB Frequency [Hz]	
	Experimental	Numerical	Experimental	Numerical
1st (translation in Y)	12.07	13.51	10.30	14.73
2nd (translation in X)	11.55	12.62	7.41	13.77
3rd (torsional)	16.27	20.22	18.25	22.35

Table 4: Correlation between experimental and numerical results

With reference to the URB the correlation between numerical and experimental results is good enough (variations in the order of the 10%) to dictate the validity of the FE model. On the contrary for the REB building the difference is quite significant (variation up to 85% on the 2nd natural frequency). The reason comes from the fact that the stone building before being reinforced has been damaged and this damage has not been quantitatively identified while also the crack patters was not defined. The uncertainties in modeling the existing damage probably caused the not perfect fit between the numerical and the experimental results for the REB. This suggests that a quantification of the damage can be achieved by only micro-scale simulations of the reinforcement as will be presented in chapter 4 of this paper. The preliminary model, with reference to modal analysis, can be considered suitable in defining a reference framework where optimized models can be conceived.

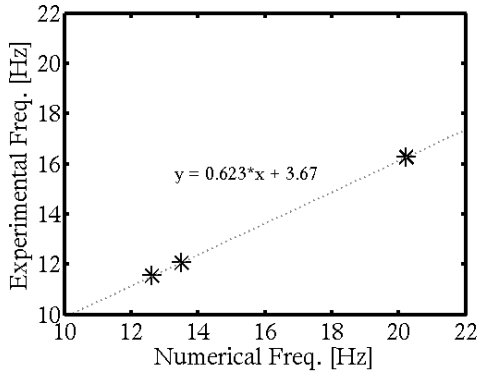

Figure 10: Correlation between experimental and numerical natural frequencies for the URB

3.2 Non-Linear Static Analysis

A non-linear static analysis (pushover) has been carried out to identify the crack patterns and to predict the damage propagation of both the URB and the REB. A distribution of forces proportional to the mass of the building is applied in the longitudinal direction at the level of the first slab and of the wood roof. The force is incrementally increased till the failure level of the stone material is reached. The Solid65 element has been adopted to model the walls stones as it provides the capability to identify the propagation of cracks during the application of the load, as it is suitable for treatment of nonlinear material properties. The element allows cracking in three orthogonal directions, crushing, plastic deformation, and creep. Bilinear stress-strain tension-compression behavior is adopted to simulate the mechanical behavior of the stone elements.

The aim of the analysis for the URB is to show the crack patterns at failure in order to provide a reference case for the simulation of the reinforced building. This allows understanding the benefit in terms of cracks propagation due to the adoption of full-cover reinforcement. In fact, as done for the URB, a pushover analysis has been carried on for the REB. The forces herein applied account for the textile mass.

Figure 11 below reports the results of the simulation for both the URB (top plots) and the REB (bottom plots). In detail the results are depicted in terms of crack patterns (left plots); and plastic strain distribution (right plots).

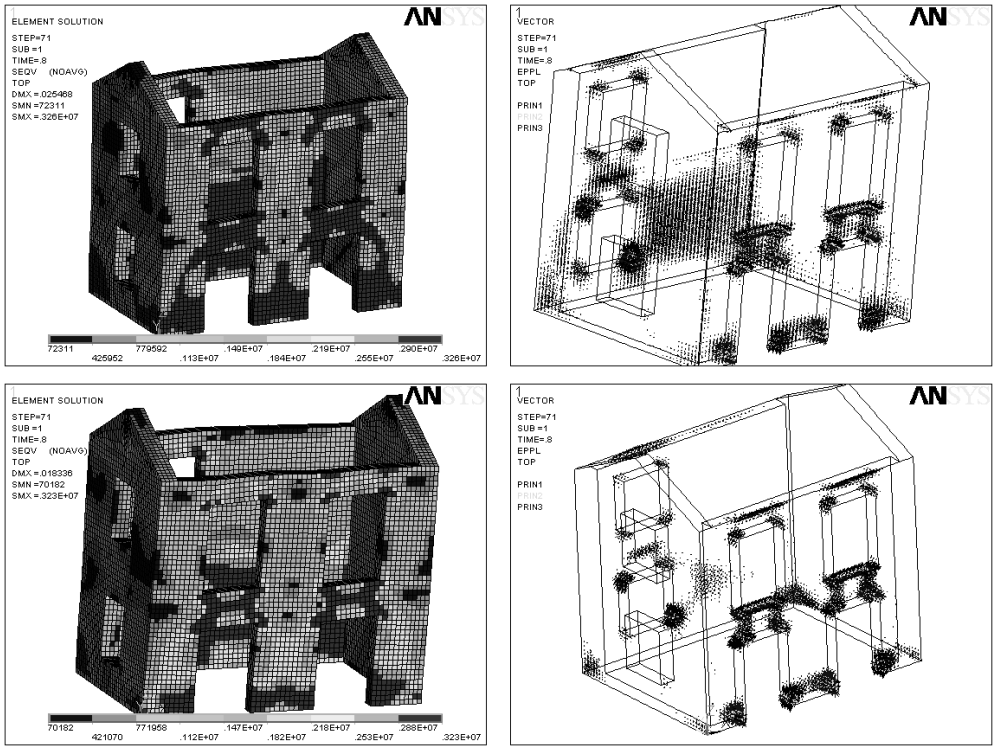

Figure 11: Pushover analysis results of the URB (top) and the REB (bottom): crack patterns at failure (left plots), plastic strain distribution (right plots)

From Figure 11 it is clear that in terms of plastic strain, a reduction in terms of their amplitude could be reached by the REB with respect to the URB.

To better understand how the reinforcement is modifying the buildings mechanics, a comparison in terms of stress-strain diagram of a control node (located at the top of the frontal wall façade) is given in Figure 12. This allow for quantifying the increase in ductility the REB has been claimed within this paper to give.

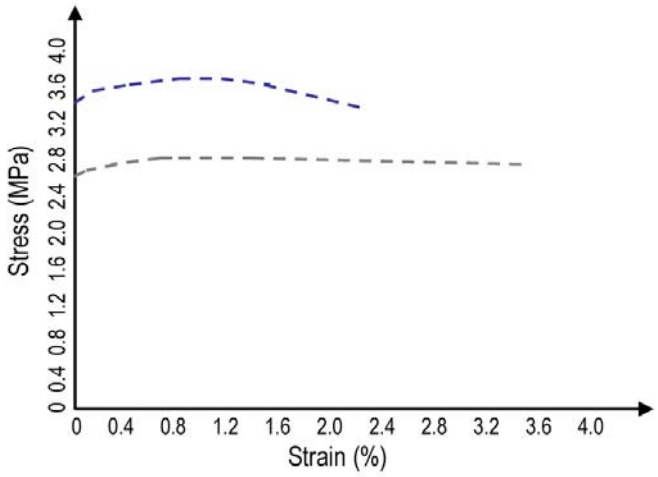

Figure 12: Stress and strain diagram of the control node for the URB (blue line) and the REB (grey line)

The REB building exhibits an elastic-plastic behavior with an increase in ductility which is evident by looking at the stress-strain plot in the post-yield field: a decreasing slope corresponding to a brittle material behavior is shown on the top right plot, while a linear horizontal trend (i.e. ductile behavior) is shown by looking at the diagram of Figure 12.

From the pushover analysis it is shown that the full-cover reinforcement allow for accounting a reduction of plasticity and an increase in ultimate strength and ductility of the stone building.

3.3 Non-Linear Dynamic Analysis

Dynamic analyses have been carried out to simulate the building response in its two configurations (URB and REB) under dynamic loads, as those of seismic events. The aim here is to assess in terms of stress-strain distribution the effects of the reinforcement solution.

A series of accelerogram, of increasing intensity, have been simulated. The Montenegro accelerogram scaled at different value of Peak Ground Acceleration (PGA) has been used. It refers to the Montenegro Earthquake happened the 19th of April 1979, with a Magnitude (Ms) of 7.0 and a PGA of 0.22g.

For simplifying the numerical simulations and in accordance to the implicit FE approach (as developed within the Ansys software) instead of a base acceleration, a base displacement is applied to the base nodes of the model. An example of the base displacement time history (referring to the Montenegro accelerogram scaled at 0.1g of PGA) is given in Figure 13 below.

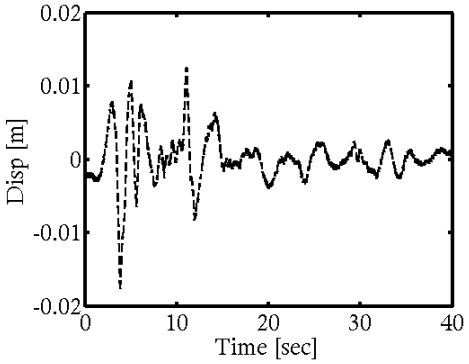

Figure 13: FE dynamic analysis: input displacement time histories referring to the Montenegro accelerogram with PGA scaled to 0.1g

The field vector of the principal stress distribution and the plastic stress distribution at critical time (12.1sec) are chosen as output parameters to be used as a source of comparison in between the URB and the REB results. They allow quantifying the benefits in terms of reduction of the limit stress amplitude and of redistribution (i.e. a more uniform configuration) of the stress field vector due to the full-cover reinforcement. Figure 14 reports these outputs for both the URB (top plots) and the REB (bottom plots).

From Figure 14, it arises that a significant reduction of the plastic strain amplitude is achieved by means of the reinforcement. This is particularly true for the front transversal walls. The beneficial effect of this reduction is obtained thanks to the confinement effect of the full-cover textile reinforcement and to its ability of increasing the building resistance to dynamic loads.

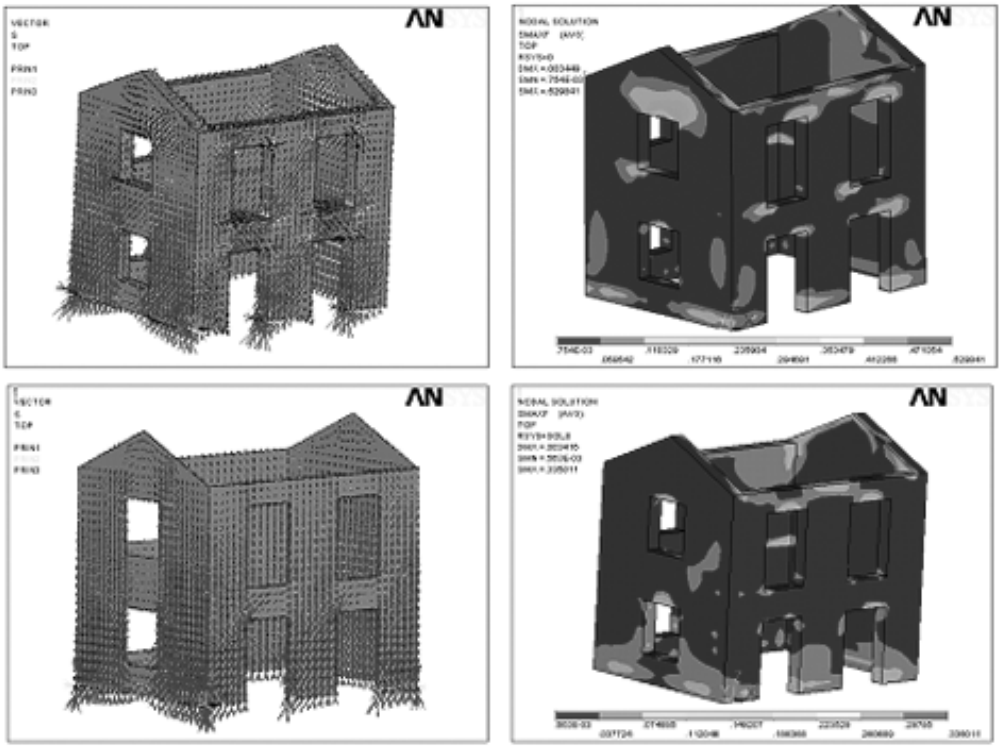

Figure 14: FE dynamic analysis: stress field vector distribution (left) and plastic stress distribution (right) at critical time

4 HEURISTIC TOOL FOR THE SIMULATION OF THE TEXTILE BEHAVIOUR

For the proper simulation of the inelastic behavior of this innovative textile an evolutionary approach will be implemented. This process utilizes Genetic Algorithms (GAs) as the optimizing tool for the identification of the parameters that govern the multiaxial polymer material behavior. This heuristic tool has been chosen for this problem since in contrast to gradient based approaches GAs do not require a straightforward analytical relationship connecting the function to be optimized to the design parameters of the problem. Instead, they can handle even loosely defined problems. A meso-scale approach will be followed, where a finite element algorithm (ANSYS) is used for the simulation of the model structure. The parameters to be identified involve both the setup of the finite element characteristic volume chosen to simulate the polymer textile, i.e. number of layers, thickness, layout, as well as the polymer and masonry material properties, i.e. Elasticity modulus, ultimate strength, etc. This constitutes the setup of the forward problem (Figure 15) which will have to be iteratively solved as part of the evolutionary cycle until convergence is achieved to a minimal error between the experimentally observed and the numerically computed behavior.

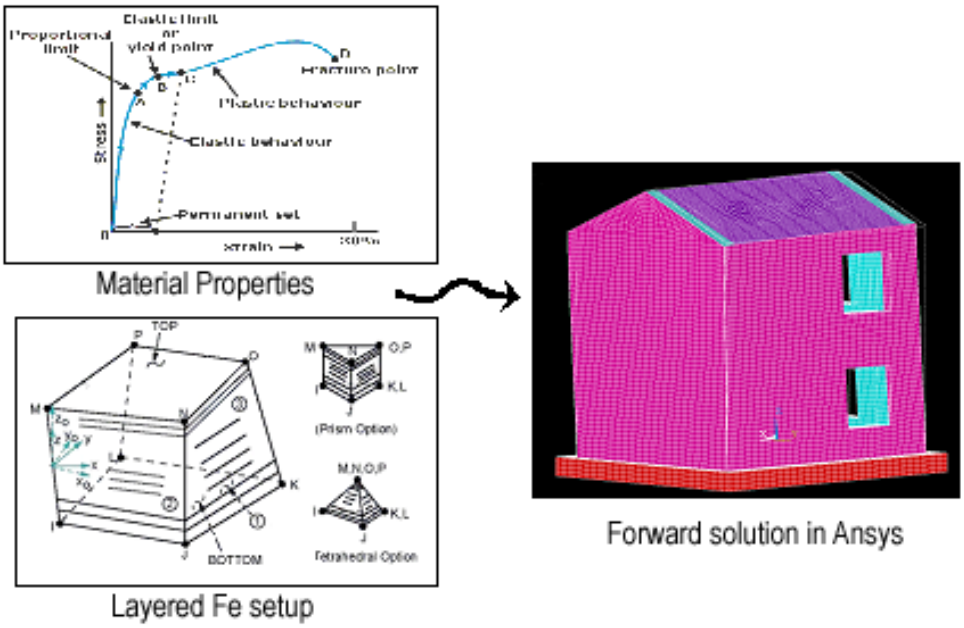

Figure 15: Forward Run

All genetic algorithms are based on the following scheme:

4.1 Representation

Depending on the application the parameters of the problem can be either integer or real numbers. Usually, the set of parameters can be appropriately encoded into a finite length binary string. Once a representation is decided a number of different chromosomes is randomly generated to form the initial population.

4.2 Fitness evaluation/selection

The evaluation of the fitness for each member of the population is carried out through the use of an objective function associated with each problem. The suitability of each chromosome is the criterion based on which this individual will be selected for reproduction. Selection can be

performed through various schemes like “roulette wheel” selection or “tournament” selection. The roulette wheel selection is solely dependent upon the performance (fitness) of each individual. In the case of the second method, the probability of a string selection is also dependent upon the fitness of the “competitive” strings chosen to participate in a tournament round. The latter contributes toward the preservation of the diversity of the population.

4.3 Crossover

This operator is applied with a certain probability, to the pairs of the previously selected individuals (parents). In general the crossover procedure randomly selects a position in the binary string and mutually exchanges the parts of the chromosome before and after this location in order to produce two offsprings.

4.4 Mutation

The use of the crossover procedure as the only means for generating new individuals could result in the loss of the diversity of the population. This problem can be overcome using the mutation operator which involves the random flip of the binary genes of the chromosome for the case of jump mutation, or the alteration of the phenotypic (real) representation of the design parameters by a small increment or decrement for the case of creep mutation. More information on the basic (classic) GA scheme can be found in [10]-[14]. The following figure illustrates the basic workings of the GA-FE optimization scheme.

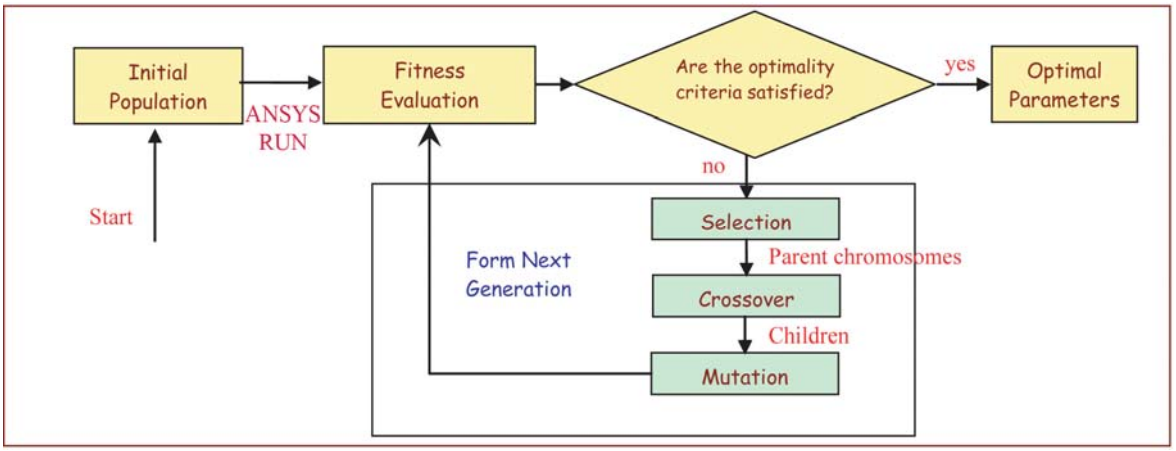

Figure 16: GA-FE Scheme

On a first level, the experimental modal analysis results listed in Table 4 for the Unreinforced Structure will serve as a reference for the calibration of the masonry material properties. On a second level the experimental modal frequencies of the Retrofitted Structure will serve as a reference for the calibration of the polymer elastic properties as well as the representative volume configuration. The error function used to evaluate the fitness of each potential set of parameters in both cases is expressed as the L_2 relative error norm:

$$r = \frac{\left\| \lambda_e - \lambda_m \right\|}{\left\| \lambda_m \right\|} \tag{1}$$

Where λ_e is the GA estimated eigenvalue vector and λ_m is the experimentally determined one. Finally, the acceleration and strain history results from the shake table test number 3, af-

ter which failure was originally noted will serve as the basis for the proper configuration of the masonry and polymer textile ultimate strength properties.

A full transient time history analysis is generally computationally expensive; therefore a response spectrum analysis will serve as the tool for the forward problem solution in this final stage, cutting down significantly on the computational cost. The fitness function in this case will be defined as the L_2 relative error norm of the maximum displacements and trains obtained from the FE Response Spectrum analysis as compared to the experimentally observed ones during the shake table test.

The finally identified parameters will ultimately be validated using a full on transient time history analysis the results of which will be compared to the actually recorded acceleration and train records at the available sensor locations.

5 DAMAGE DETECTION BY MEANS OF STRAIN MEASUREMENTS

An experimental tests campaign has been carried on aimed at detecting the REB dynamics by means of FBG sensors embedded textile. Hammer tests were performed after each simulated seismic event as reported in Table 5.

Test	Description
1	Modal identification after the 1st seismic test (Montenegro accelerogram scaled to 0.1g of PGA)
2	Modal identification after the 2nd seismic test (Montenegro accelerogram scaled to 0.3g of PGA)
3	Modal identification after the 3rd seismic test (Montenegro accelerogram scaled to 0.4g of PGA)
4	Modal identification after the 5th seismic test (Montenegro accelerogram scaled to 0.6g of PGA)

Table 5: Experimental modal identification tests chronology

The sensor topology was chosen as shown in Figure 17: a total of 8 FBG sensors (active length of 2m) have been installed on Wall1, 2, 3 and 4. The excitation point is also depicted with a red arrow in Figure 17.

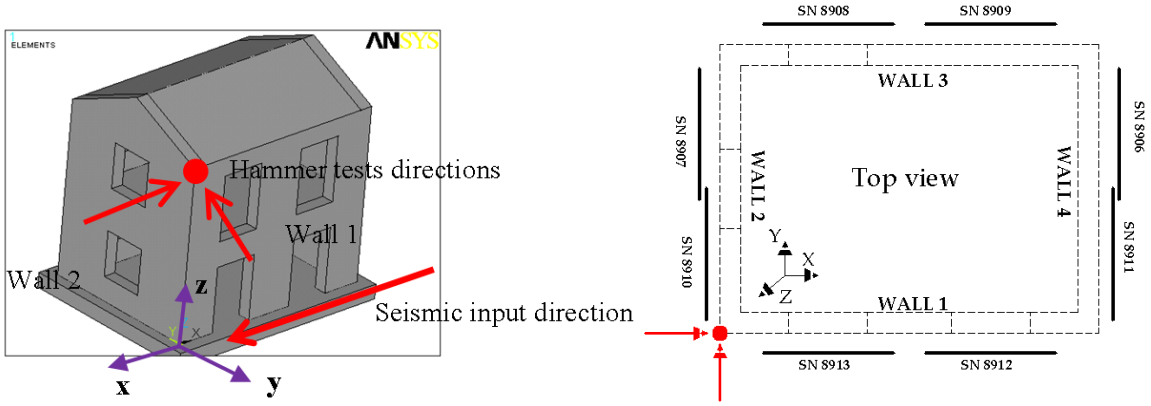

Figure 17: Experimental modal identification tests set-up: 3D view (left); plane view (right)

For each test, two hammer trials along X-direction and two along Y-direction have been conducted. From the data recorded by FBG sensors an Operational Modal Analysis (OMA) has been carried by adopting the ERA algorithm.

For seek of brevity in what follows only the most significant results (for test1 and test4) are depicted in the time (strain Time History) and frequency (Power Spectral Density function – PSD) domain. Singular Values Decomposition (SVD) plots are also showed. Table 6 summarizes the results in terms of identified natural frequencies.

Each sensor records the structural response in terms of axial strain, sampling at 1000Hz, manually down-sampled at 100Hz. Such sampling frequency defines a frequency range 0-50Hz (according to the Nyquist theorem) which is good enough to detect the building natural frequencies, as dictated by the FE modal simulations.

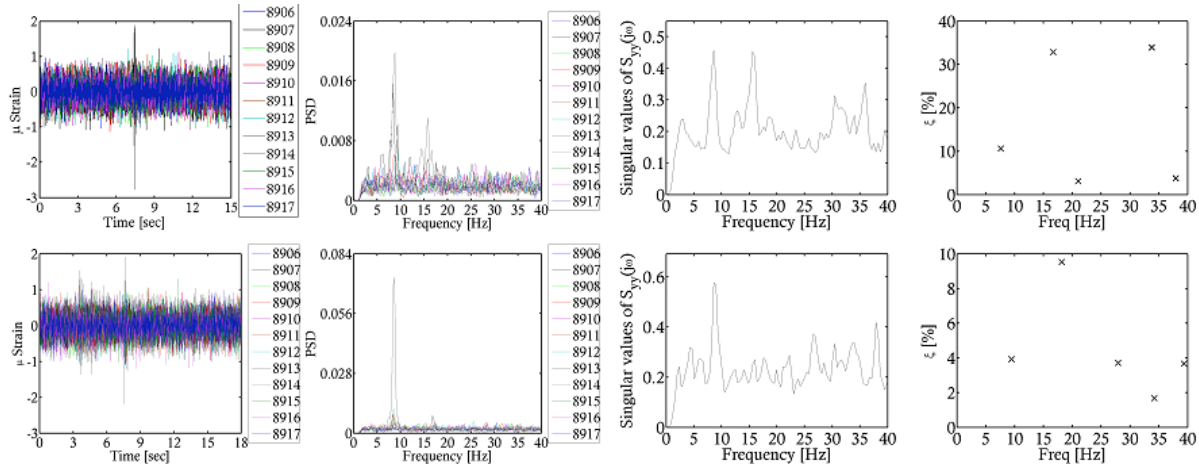

Figure 18: Test1 results for the hammer tests along X (top) and hammer tests along Y (bottom). Calculated displacements Time History (left plot), Power Spectral Density function (middle left plot); Singular Values as obtained by the SVD of the PSD matrix (middle right plot); Identified frequency vs. identified damping from Next-ERA algorithm (right plot)

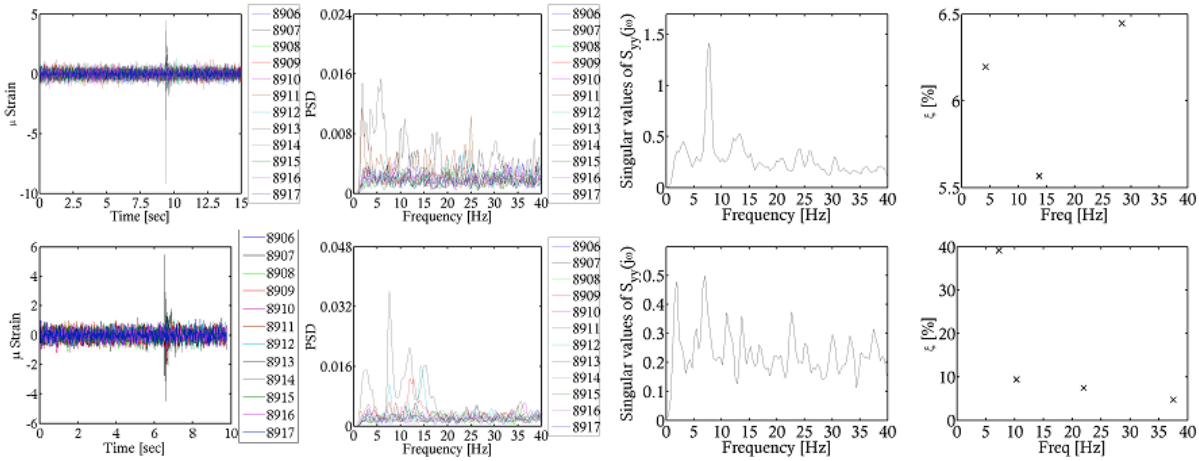

Figure 19: Test4 results for the hammer tests along X (top) and hammer tests along Y (bottom). Calculated displacements Time History (left plot), Power Spectral Density function (middle left plot); Singular Values as obtained by the SVD of the PSD matrix (middle right plot); Identified frequency vs. identified damping from Next-ERA algorithm (right plot)

Mode	Test1 (1st seismic test) Freq. [Hz]	Test2 (2nd seismic test) Freq. [Hz]	Test3 (3rd seismic test) Freq. [Hz]	Test4 (5th seismic test) Freq. [Hz]
First mode (Y)	8.98	8.88	12.42	8.98
Second mode (X)	7.60	8.07	7.86	7.78
Third mode (tors)	15.39	15.49	13.92	13.86

Table 6: Identified natural frequencies

To define the evolution/variations of the building natural frequencies from Test1 to Test4, Figure 20 depicts the SVDs as calculated for the hammer tests in the X and Y direction respectively. This graph gives an idea of how, at least for the 1st and the 2nd mode, the natural frequencies associated to translational modes of the building (1st in Y direction, 2nd in X direction) varies according to the different structural configuration of the building after each seismic test.

It is worth noting, as not mentioned previously that some considerations may be done, based on the measurements recorded during the seismic tests, on the structural changes of the stones building and on the development of a progressive failure condition. These following considerations are strongly related to what it is expended to extract from the hammer tests data in terms of frequencies and then of damage detection. In other words if a failure is locally and/or globally identified after a seismic event, this has to corresponds to changes in the building dynamics (i.e. variation of natural frequencies). To understand if a correlation is possible the following considerations should be preliminary highlighted:

- After the 1st seismic test (PGA 0.1g) the #REB was not affected by any damage, the structure resists to the dynamic force easily and not visual damage was detected. From the data processing, no plastic (i.e. permanent) deformation was measured;
- After the 2nd seismic test (PGA 0.3g) the #REB was not affected by any evident damage and no plastic deformations were detected;
- After the 3rd seismic test (PGA 0.4g) the #REB was affected by structural damage which mainly occurred at the top of the windows of wall2, where sensors SN8912 and SN8913 were installed. From the data processing of the measurements recorded during the seismic test, plastic strains were detected;
- After the 4th seismic test (PGA 0.5g) the #REB, localized damage by the 3rd test, was able to respond with no apparent further cracks. No additional plastic deformation was recorded;
- After the 5th seismic test (PGA 0.6g) the #REB was able to resist to the strong seismic shake with evident damages which were globally located on the building walls (above all on Wall1). Additional and significant plastic deformations were recorded during the seismic test. A damaged configuration seems to be the more appropriate to describe the #REB after the 5th test.

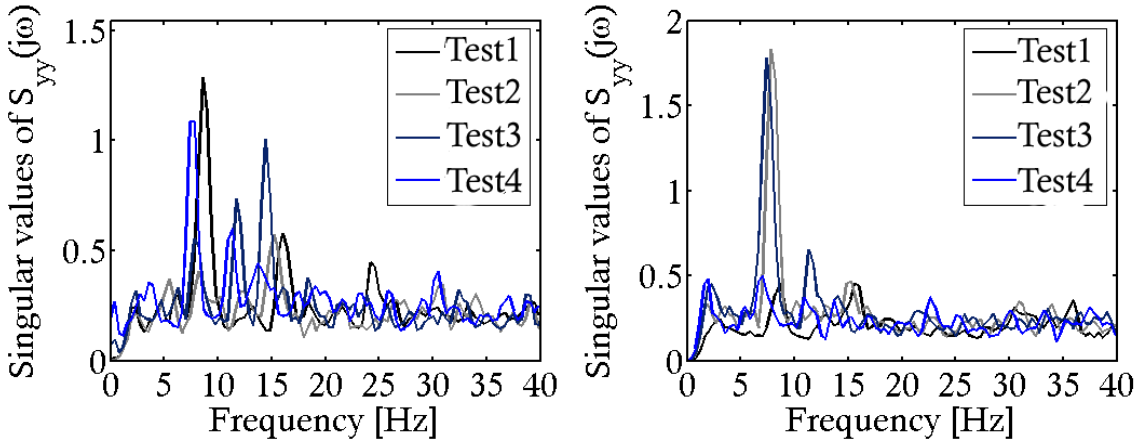

Figure 20: Tests 1-4 system identification results: Singular Values as obtained by the SVD of the PSD matrix for the hammer tests in X direction (left), in Y direction (right)

From Figure 20 some trends may be evidenced in terms of 1st in X and 1st in Y (see blue and black lines at the first peak) natural frequencies variations from test1 to test4. Figure 21 highlights them by separating the SVD graphs obtained for Test1 to those of Test4. The values of the natural frequencies depicted in Figure 21 are reported in Table 7 below.

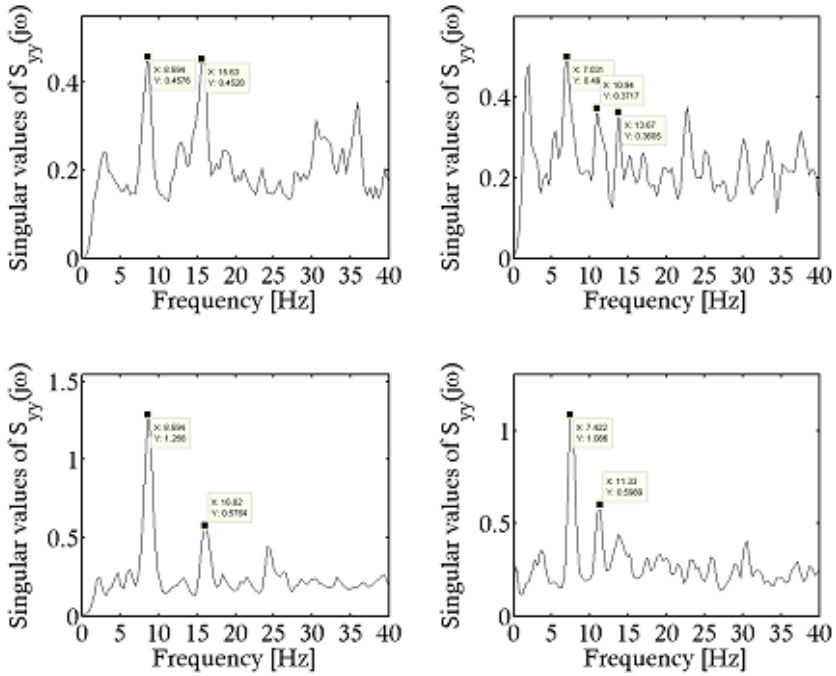

Figure 21: Tests 1-4 system identification results: Singular Values as obtained by the SVD of the PSD matrix for the hammer tests in X direction (top) and in Y direction (bottom): Test1 results (left), Test4 results (right)

From Figure 21 it can be noted that:

- the 1st first mode natural frequency decreases from 8.59Hz to 7.81Hz, which means a reduction of the 9.1%. This indicates also for the building natural movements along the transversal direction (Y axis) that the building stiffness decreased from the 1st to the 5th seismic test, due to cracks opening into Wall2;

- the 2nd mode natural frequency decreases from 8.59Hz to 7.03Hz, which means a reduction of the 18.2% X. This indicates that the REB was either less stiff or its weight was increased after the last seismic test than after the 1st seismic test. As no mass was added, the building after five subsequent seismic tests was less stiff due to cracks openings in localized positions. In addition this was also due to an out-of-plane mechanism of Wall1 along the longitudinal direction (X-axis).

	Test1 (after the 1st seismic test) Freq. [Hz]		Test4 (after the 5th seismic test) Freq. [Hz]	
	First mode (Y)	Second mode (X)	First mode (Y)	Second mode (X)
FBG sensors	8.59	8.59	7.81	7.03

Table 7: Identified natural frequencies for test1 and test4 from SVD

6 CONCLUSIONS

Sensor-embedded reinforcing textiles offer the engineer a new tool for the retrofit of masonry structures. These multifunctional materials reinforce and monitor in one product. As such, they strengthen, reduce seismic risk, and provide the engineer with data that can be utilized to assess a structure in all phases of its life cycle.

The "Composite Seismic Wallpaper", described along this paper, is an innovative example of such type of multifunctional materials. The main outcomes from an experimental tests campaign, as well as the main results of numerical investigations have been here detailed. The objective was to furnish elements for the validation of the performance of the wallpaper as seismic reinforcement of masonry buildings.

The characterization of the wallpaper behavior is highlighted in Chapter 4, while its ability to be used as a tool for damage detection of cracks in the reinforced structure is reported in Chapter 5.

REFERENCES

[1] T. B. Messervey, D. Zangani, C. Fuggini, Sensor-embedded textiles for the reinforcement, dynamic characterisation, and structural health monitoring of masonry structuress, *Proceedings of the 5th EWSHM 2010*, June 28–July 2, 2010, Sorrento, Italy, pp. 1075-1282.

[2] Faella C, Martinelli E, Nigro E, Paciello S, Tuff masonry walls strengthened with a new kind of C-FRP sheet: experimental tests and analysis. *Proceedings of the 13th world conference on earthquake engineering*, paper no. 923, 2004.

[3] Krevaikas T, Strengthening of unreinforced masonry structures with advanced composites. *PhD Dissertation*, University of Patras, Greece, 2005.

[4] Nurchi A, Valdes M, Strengthening of stone masonry columns by means of cement-based composite wrapping. *Hamelin P (ed) CCC 2005: 3rd international conference on composites in construction*. Lyon, France, July 2005, pp 1189–1196

[5] Triantafillou TC, Fardis MN, Strengthening of historic masonry structures with composite materials, *Material Structure*, 30, 486–486, 1997.

[6] Krevaikas T, Triantafillou TC, Masonry confinement with fiber reinforced polymers. *J Compos Constr*, 9(2), 128–135, 2005.

[7] Krevaikas TD, Triantafillou TC, Computer aided strengthening of masonry walls using fibrereinforced polymer strips. *Mater Struct* 38, 93–98, 2005.

[8] Li T, Galati N, Tumialan JG, Nanni A, Analysis of unreinforced masonry concrete walls strengthened with glass fiber-reinforced polymer bars, *ACI Struct J*, 102(4), 569–577, 2005.

[9] CNR-DT 200/2004: Guide for the Design and Construction of Externally Bonded FRP Systems for Strengthening Existing Structures

[10] D. Whitley, A genetic algorithm tutorial, Stat Comput **4** (1994), p. 6585.

[11] B.L. Miller, B.L. Miller and D.E. Goldberg, Genetic algorithms, tournament selection, and the effects of noise, Complex Syst **9** (1995), pp. 193–212.

[12] Goldberg DE. Sizing populations for serial and parallel genetic algorithms, In: Proceedings of the 3rd International conference on genetic algorithms, Morgan Kaufman; 1989. p. 70–9.

[13] M. Mitchell, An introduction to genetic algorithms, MIT Press, Cambridge, MA (1998).

[14] T. Back, D.B. Fogel and Z. Michalewicz, Handbook of evolutionary computation, IOP Publishing Ltd, Bristol, UK (1997).